Title
Nf-GH, a glycosidase secreted by Naegleria fowleri, causes mucin degradation: an in vitro and in vivo study.

Journal
Future Microbiology, 12(9)

Authors
Martínez-Castillo, Moisés
Cárdenas-Guerra, Rosa
Arroyo, Rossana
et al.

Publication Date
2017-07-01

DOI
10.2217/fmb-2016-0230

Peer reviewed

RESEARCH ARTICLE

For reprint orders, please contact: reprints@futuremedicine.com

Future MICROBIOLOGY

Nf-GH, a glycosidase secreted by *Naegleria fowleri*, causes mucin degradation: an *in vitro* and *in vivo* study

Moisés Martínez-Castillo[1], Rosa Elena Cárdenas-Guerra[1], Rossana Arroyo[1], Anjan Debnath[2], Mario Alberto Rodríguez[1], Myrna Sabanero[3], Fernando Flores-Sánchez[4], Fernando Navarro-Garcia[4], Jesús Serrano-Luna[4] & Mineko Shibayama*[,1]

Aim: The aim of this work was to identify, characterize and evaluate the pathogenic role of mucinolytic activity released by *Naegleria fowleri*. **Materials & methods:** Zymograms, protease inhibitors, anion exchange chromatography, MALDI-TOF-MS, enzymatic assays, Western blot, and confocal microscopy were used to identify and characterize a secreted mucinase; inhibition assays using antibodies, dot-blots and mouse survival tests were used to evaluate the mucinase as a virulence factor. **Results:** A 94-kDa protein with mucinolytic activity was inducible and abolished by p-hydroxymercuribenzoate. MALDI-TOF-MS identified a glycoside hydrolase. Specific antibodies against *N. fowleri*-glycoside hydrolase inhibit cellular damage and MUC5AC degradation, and delay mouse mortality. **Conclusion:** Our findings suggest that secretory products from *N. fowleri* play an important role in mucus degradation during the invasion process.

First draft submitted: 16 December 2016; Accepted for publication: 7 April 2017; Published online: 13 June 2017

KEYWORDS
• glycosidases • mucinases
• mucins • *Naegleria fowleri*
• secretory products

Naegleria fowleri is a free-living amoeba that enters the nasal cavity and migrates to the brain, causing primary amoebic meningoencephalitis (PAM) in humans. Diverse pathogenic mechanisms such as adhesion [1,2], locomotion [3], phagocytosis [4,5] and protease activity [6–9] have been described for *N. fowleri* trophozoites. It is possible that these mechanisms have an important role in the infection process. Immunohistochemical studies of the early stages of PAM infection in a murine model have shown that the amoebae induce mucus secretion and an inflammatory reaction in the nasal cavity [10,11].

The nasal epithelial mucus is mainly composed of mucins (secreted mucins MUC5AC, MUC5B and MUC2) that are essential for maintaining the sterility of the microenvironment in the upper airway [12]. Mucins are complex glycoproteins that can be associated with the cellular membrane or released to form a polymeric gel [13]. The biochemical structure of these proteins consists of a central region with variable numbers of tandem repeat regions (VNTR). The genes of VNTR regions are used to differentiate mucin family members (20 members in humans) [12,14]. Serine (Ser), threonine (Thr) and proline residues present in VNTR regions are O-glycosylated in the Golgi apparatus,

[1]Department of Infectomics & Molecular Pathogenesis, Center for Research & Advanced Studies of the National Polytechnic Institute, Av IPN 2508, Mexico City 07360, Mexico
[2]Center for Discovery & Innovation in Parasitic Diseases, Skaggs School of Pharmacy & Pharmaceutical Sciences, University of California San Diego, La Jolla, CA 92093, USA
[3]Department of Biology, University of Guanajuato, Noria Alta S/N, Noria Alta, Guanajuato 36050, Mexico
[4]Department of Cell Biology, Center for Research & Advanced Studies of the National Polytechnic Institute, Av IPN 2508, Mexico City 07360, Mexico
*Author for correspondence: Tel.: +52 555 747 3348; Fax: +52 555 747 3398; mineko@cinvestav.mx

Future Medicine part of fsg

with up to 80% carbohydrate constituting the total weight of mucin proteins [14]. Glycosylation confers specific charge and hydrophobicity to mucins and is related to its resistance to physical or biochemical injury [13,14]. It has been reported that *Entamoeba histolytica* exhibits glycosidase activity that can degrade mucin oligosaccharides. Similarly, secretion of proteases for *E. histolytica* has been related to intestinal mucin degradation (MUC2) [15–17]. Degradation of mucins by secretory products (SPs) has been described for other mucus-dwelling protozoa, such as *Tritrichomonas foetus*, *Giardia lambia* and *Trichomonas vaginalis* [18]. Proteins detected in the SPs of these microorganisms include sialidases, glycosidases and cysteine proteases [15,16,18]. It is important to mention that mucinolytic activity refers the degradation of mucins by any molecule that includes proteases and other enzymes, whereas proteolytic activity is a general terminology that involves the degradation of proteins.

Several studies have been performed to determine the activity of *N. fowleri* proteases and their specific host substrates, which may include myelin, immunoglobulins, iron-binding proteins and collagen [8,9,19,20]. However, very few studies have been performed in *Naegleria* to identify and purify secreted proteases [6,8]. Recently, our group demonstrated that trophozoites and total crude extracts of *N. fowleri* can degrade the MUC5AC mucin protein. However, molecular identification of the proteolytic enzymes has not yet been achieved [21].

We decided to identify and explore the role of mucinolytic molecules in the SPs of *N. fowleri* as a mechanism to evade the mucus of the olfactory mucosa, which is part of the innate immune response. Initially, we determined whether *N. fowleri* releases mucinolytic proteins. In addition, partial biochemical characterization of mucinases was performed using different protease inhibitors. The results revealed that the inhibitors p-hydroxymercuribenzoate (pHMB), phenyl-methyl sulfonyl fluoride (PMSF) and aprotinin have the capacity to inactivate these mucinolytic activities. The mass spectrometry analysis allowed us to identify a glycoside hydrolase (GH) in *N. fowleri*; moreover, the use of specific carbohydrates as substrates was employed to distinguish the type of enzymatic activity by the GH. Likewise, we designed a peptide similar in structure to the active domain of a GH and obtained specific antibodies against the GH of *N. fowleri* (Nf-GH). These antibodies were employed to protect against the degradation of human MUC5AC induced by the SPs of *N. fowleri*. Finally, *in vivo* studies using trophozoites preincubated with anti-GH antibodies showed that the survival of mice was extended for 10 days compared with mice infected with untreated amoebae. Thus, *N. fowleri* glycosidases may be involved in human mucus degradation during the first stage of PAM progression.

Materials & methods

• Cell cultures

A pathogenic strain of *N. fowleri* (ATCC 30808) was maintained under axenic conditions in 2% bactocasitone medium supplemented with 10% (v/v) fetal bovine serum (FBS; Equitech-bio, Kerrville, TX, USA) at 37°C. To maintain virulence, trophozoites (2×10^4) were instilled in mice. 7 days postinfection, the brains were recovered in bactocasitone medium (Becton and Dickinson; Sparks, MD, USA) with streptomycin/penicillin (Gibco, NY, USA), as previously reported [22,23].

Mucoepithelial cells (NCI-H292; ATCC: CRL1848) were grown in RPMI 1640 (Gibco, Invitrogen, NY, USA) with 10% FBS (v/v; Equitech-bio, TX, USA) in a 5% CO_2 atmosphere at 37°C. The cells were grown until confluence. To obtain secreted MUC5AC mucin, the cells were incubated with serum-free medium with 20 nM PMA (Phorbol 12-Myristate 13-Acetate; Sigma-Aldrich, MO, USA) for 24 h, and supernatants were centrifuged at 1500 × *g* for 10 min. The supernatant containing mucins was concentrated with Amicon ultrafilters (cut-off: 100 kDa) and stored at 70°C until use.

• Animal-management protocols

The animal-management protocols were approved by the institutional committee (IACUC). BALB/c mice at 3–4 weeks of age were used for virulence tests and survival experiments (ID number 0071-13). New Zealand male rabbits (2 weeks old) were used for antibody development (ID number 0414-08). Our institution fulfills all technical specifications for the production, care and use of laboratory animals and is certified by national law (NOM-062-ZOO-1999). Animals were euthanized with an overdose of sodium pentobarbital at the end of the experiments and handled according to the guidelines of the 2000 AVMA Panel on Euthanasia.

• Sample preparation

Trophozoites (6×10^6) were grown until logarithmic phase (48 h), and the medium was replaced with serum-free bactocasitone medium. After 12 h, the amoebic SPs were collected from viable trophozoites by removing complete trophozoites and cellular debris by centrifugation at 1500 × *g* for 10 min; trophozoite cell viability was determined using SYTOX green (Molecular Probes, TX, USA). The supernatant containing the SPs was passed through a 0.22-µm Durapore membrane (Millipore, MA, USA). SPs from the supernatants were precipitated with absolute ethanol (JT Baker, PA, USA) at a 3:1 ratio for 1 h at -20°C, after which the samples were centrifuged at 6500 × *g* for 45 min. The pellet containing SPs was suspended in 1 ml of Tris-HCl (20 mM; pH 8.0; Sigma-Aldrich), and the samples were stored at 4°C until the ethanol evaporated (12 h). The protein concentration of ethanol-treated SPs was quantified according to the Bradford method [24].

• Proteolytic & mucinolytic activities by substrate gel electrophoresis

The protease activities of the SPs and ethanol-treated SPs were determined by zymography assays using 10% polyacrylamide copolymerized with porcine gelatin (Sigma-Aldrich) or bovine submaxillary mucin (BSM; Worthington Biochemical Corporation, Lakewood, NJ, USA) to a final concentration of 0.1% for both substrates. 40 µg of total protein from samples was loaded. As an experimental control, 30 µl of bactocasitone medium precipitated with ethanol was used. Electrophoresis was performed at a constant voltage (80 V) for 3 h in an ice bath (4°C); the gels were then washed two-times for 30 min with agitation in a 2.5% (v/v) Triton X-100 solution (Sigma-Aldrich). The zymogram gels were incubated overnight at 37°C in buffers at several pHs: 100 mM sodium acetate (pH 5.0), 100 mM Tris-HCl (pH 7.0) or 100 mM glycine (pH 9.0). All buffers contained 2 mM $CaCl_2$ and 2 mM DTT. Finally, the gels were stained with 0.5% (w/v) Coomassie Brilliant Blue R-250 (JT Baker). Protease activities were identified as clear bands on a blue background. All assays were performed in triplicate.

• Protease inhibitors

The ethanol-treated SPs were preincubated at 37°C for 1 h using various protease inhibitors with gentle agitation. The following final concentrations and types of protease inhibitors were used: for cysteine proteases, 10-mM pHMB, 10-µM (1-{*N*-[(L-3-trans-carboxyoxirane-2-carbonyl)-L-leucyl]amino}-4-guanidinobutane [E-64]), 5-mM n-ethylmaleimide (NEM) and 5-µM iodoacetamide (IAA); for serine proteases, 5 mM PMSF and 1 mM aprotinin; for metalloproteases, 10-mM 1,10-phenanthroline [25] (Sigma-Aldrich). All the zymograms were activated at pH 7. Zymography assays were performed to evaluate the effect of each inhibitor tested. Inhibition analyses were performed by densitometry analysis using the ImageJ program [26], and the results are expressed as relative optical density (ROD).

• Stimulation of mucinases with BSM

6 million *N. fowleri* trophozoites were incubated in serum-free medium for 3 h. These trophozoites were then incubated with BSM dissolved in serum-free medium (0.1 mg/ml) for 1, 3, 6 and 12 h. After incubation, SPs were obtained and precipitated with ethanol (JT Baker) at a 3:1 ratio, as previously described. As an experimental control, ethanol-treated SPs from trophozoites incubated in serum-free medium without mucin were used for the same time periods. The samples were stored at -70°C until use.

• Anion exchange chromatography

Ethanol-treated SPs were applied to a 1 ml anion exchange resin High-Q cartridge (Bio-Rad, CA, USA), which had been previously equilibrated at room temperature with 20 mM Tris-HCl buffer at pH 8.5. The samples were loaded and incubated overnight at 4°C. Elution was performed using a discontinuous gradient of equilibration buffer containing 0.1, 0.2, 0.3, 0.4 and 0.5 M NaCl (0.5 ml/min). Each fraction collected was assayed, analyzed by SDS-PAGE and tested for mucinolytic activity using zymography. Fractions of 1 ml showing the maximum activity were concentrated and desalinated with Amicon ultrafilters (cut-off: 100 kDa). This fraction was designated the mucinase-enriched fraction (MEF). The samples were stored at -70°C until use.

• Protein identification by mass spectrometry

The mucin-inducible mucinase with a size of 94 kDa was further identified by mass spectrometry. Two protein bands with 94 kDa, one from a Coomassie-stained gel and another from a mucin

zymogram, were processed by tryptic digestion and analyzed by electrospray ionization mass spectrometry (MALDI-MS) at LANGEBIO, CINVESTAV-IPN, Irapuato, and by MALDI-TOF/MS at the Laboratory of Experimental Services LaNSE-CINVESTAV, Mexico; both analyses reached similar results. Protein identification of the 94-kDa band was performed by searching the NCBI database with the data acquired (MS/MS ions) using the MASCOT program [27] and the *N. gruberi* genome sequence from the NCBI web page. To achieve 95% confidence, the detection threshold was up to 1.3 coverage. All accession numbers were searched in the NCBI database to obtain the molecular weight (MW) and the amino acid sequence.

• Enzymatic assays of *N. fowleri* glycosidases

To determine the glycosidase activity in ethanol-treated SPs and the MEF, hydrolysis of carbohydrates was determined spectrophotometrically, using as substrates 4-nitrophenyl β-D-galactopyranoside, 4-nitrophenyl β-D-glucopyranoside and 4-nitrophenyl β-D-mannopyranoside. All substrates were used at 0.1 mM according to the manufacturer's instructions (Sigma-Aldrich). Ethanol-treated SPs or the MEF were incubated for 45 min at 37°C and evaluated at pH 5, 7 and 9 for each chromogenic substrate. The same samples were also treated with pHMB inhibitor before incubation with the substrates mentioned above. The enzymatic reaction was terminated with 100 mM NaOH, and the samples were evaluated using an Epoch microplate reader spectrophotometer (BioTek, Winooski, VT, USA) at 405 nm. Statistical analysis (two-way ANOVA) was performed using Systat Sigma Plot software [28]. Graphs were obtained using GraphPad Prism 5 software. The data are the means ± SEM of three independent experiments.

• Peptide design & antibody production

Using the mass spectrometry results, we searched for the amino acid sequence of the GH (GH, access number: 284096877) in the NCBI database. To obtain the 3D prediction and the active and catalytic sites, Phyre^2 software was used [29]. To select an antigenic peptide (18 aa) near the active site, we used ABCpred, Bcpred [30] and Kyte-Doolittle [31] software. The selected peptide (KRSMPMIRPLFYDFSSDE, residues 640–658) was synthesized and coupled to KLH to increase the immunogenicity of this peptide (PepMic, Co, Suzhou, China). New Zealand male rabbits were subcutaneously and intramuscularly immunized with 1 mg of the synthetic peptide–KLH and emulsified with Titer-Max Classic adjuvant (Sigma-Aldrich). Posteriorly, the animal received two boosts of the same antigen at the same concentration over an interval of 10 days. Preimmune (PI) serum was obtained before the immunization. The antibody concentration was determined using the bicinchoninic acid protein assay (Thermo Scientific, MD, USA).

• Immunodetection of GH in *N. fowleri* trophozoites

The antibodies generated against GH using synthetic peptides as the antigen were tested for GH in the MEF and trophozoites. Samples of ethanol-treated SPs and the MEF (30 μg) were separated using 10% SDS-PAGE in non-reducing conditions, electrotransferred to polyvinylidene difluoride (PVDF) membranes and blocked with 5% skim milk. The blot was incubated overnight with rabbit anti-GH polyclonal antibodies (1:2000) at 4°C. The membranes were washed three times with PBS-T (Tween, 0.05%) and incubated with an anti-rabbit HRP-labeled secondary antibody (Zymed, Rockford, MD, USA; 1:4000). Western blots (Wb) were revealed using luminol kit reagent (Santa Cruz Biotechnology, Delaware, CA, USA) and photographic Kodak film.

• Immunolocalization of GH in *N. fowleri*

Trophozoites were grown on coverslips and fixed with 4% paraformaldehyde (PFA; Sigma-Aldrich). Amoebae permeabilized with 0.2% Triton X-100 or nonpermeabilized were used. Samples were blocked with 10% FBS in PBS. Trophozoites were incubated with the rabbit anti-GH (1:100) antibody at 37°C for 1 h, followed by incubation for 1 h with anti-rabbit FITC-labeled secondary antibody (Zymed, MD, USA; 1:100). Nuclei were counterstained with propidium iodide (0.001%; Sigma-Aldrich) for 5 min. PI serum was used as a negative control. All samples were preserved using the Vectashield reagent (Vector, CA, USA). Samples were analyzed under a confocal microscope (Carl Zeiss LMS 700, Zeiss, CA, USA).

• Inhibition assay using anti-GH antibodies in NCI-H292 cells

With the aim of evaluating whether anti-GH antibodies inhibited the mucoepithelial damage induced by *N. fowleri* trophozoites, we

co-incubated amoebae with the NCI-H292 cell monolayer in the presence of the anti-GH antibody (1.5 μg/ml) after 1, 3 and 6 h of interaction. The optimal inhibitory concentration of the antibody was based on an agglutination assay as observed by light microscopy using *N. fowleri* trophozoites and different concentrations of antibodies. For inhibition assays, cell damage was observed using light microscopy, and the cell viability was assayed using SYTOX green (5 μM; Molecular probes, TX, USA). These assays consisted of mucoepithelial cells (20×10^4) co-cultured with *N. fowleri* (1:1) in RPMI medium without serum in the presence of the anti-GH antibody after 1, 3 and 6 h. The amoebae were removed at each incubation time point in an ice bath for 20 min. Nonpermeabilized treated cells were fixed with 2% paraformaldehyde for 20 min. SYTOX green was added for 10 min, and fluorescent nuclei indicated dead cells. Permeabilized normal cells treated with 0.2% Triton X-100 were used as a positive control, while nonpermeabilized untreated NCI-H292 cells were used as a negative control of fluorescence. Samples were observed with an inverted fluorescent microscope (Nikon, eclipse Ti-U, Tokyo, Japan). The images were analyzed using ImageJ software [26]; the total number of pixels of three independent images was analyzed and reported as fluorescence intensity. The significance was determined by comparing the control samples (cells without trophozoites) using two-way ANOVA with the Systat Sigma Plot 12 software [28].

• Anti-GH antibodies prevent human MUC5AC degradation

To demonstrate that the anti-GH antibodies prevent MUC5AC degradation, human MUC5AC mucin secretion was induced with 20 nM PMA and NCI-H292 cell supernatants (200 ml) were concentrated with Amicon ultrafilters (100-kDa cut-off). Proteins from supernatants were quantified using the Bradford method. To identify MUC5AC in the concentrated supernatants, samples were analyzed using 5% SDS-PAGE and staining with Coomassie blue reagent and by Wb. For the Wb, MUC5AC was identified using an anti-Mucin 5AC monoclonal antibody (Mucin 5AC 1-13M1, Abcam, MA, USA; dilution 1:1000 for 2 h), followed by incubation with the secondary antibody antimouse IgG labeled with HRP (Invitrogen, MA, USA; 1:10,000 for 1 h). Blots were revealed with a luminol kit reagent (Santa Cruz Biotechnology, CA, USA) using photographic Kodak film.

Zymograms contained the mucins released by NCI-H292 cells, which were concentrated (0.5 μg/μl) and used as substrate. Zymograms were loaded with MEF (40 μg), and the same fraction was preincubated with the anti-GH antibodies (5 μg/ml) or pHMB (10 mM). The zymograms were activated overnight at pH 7 and 37°C. Inhibition analyses were performed by densitometry using the ImageJ program [26].

To further detect MUC5AC degradation by the MEF, the supernatant from NCI-H292 was co-incubated with the MEF, and dot-blot assays were performed to observe MUC5AC degradation. Briefly, human-released mucins (0.5 μg/μl) from NCI-H292 cells were incubated with the MEF (80 μg/μl) in Tris-HCl at pH 7 at 37°C for 6 h. Proteinase K (PK; 0.2 μg/μl) was incubated with mucins from the cells for 20 min as a positive control. Additionally, the MEF was incubated with the released mucins in the presence of pHMB inhibitor (10 mM) or preincubated with anti-GH antibodies (5 μg/ml). The MEF alone was loaded as a negative control. All samples were dropped onto nitrocellulose membranes (0.45 μm) and stained with Ponceu's solution (Sigma-Aldrich) to visualize the bound protein. Dot-blots of each condition were determined using an anti-Mucin 5AC monoclonal antibody (1:500) for 2 h, followed by incubation for 1 h with antimouse IgG labeled with HRP as a secondary antibody (Invitrogen, CA; 1:10,000). The blots were revealed with luminol kit reagent (Santa Cruz Biotechnology) using an Odyssey FC imaging system (LI-COR, NE, USA). Densitometry analyses were performed using the ImageJ program [26], and the results were expressed as ROD.

• Delay of mouse mortality by *N. fowleri* trophozoites preincubated with GH antibodies

Mouse mortality was analyzed using various doses of *N. fowleri* trophozoites (6, 12 and 25×10^4). We used 1-month-old BALB/c mice that weighed approximately 15 g. Groups of six animals were used for each condition. Because all tested doses caused mouse mortality at 7 days postinstillation, 12×10^4 trophozoites were used in posterior experiments. Group 1 infected animals were lightly anesthetized in an ether chamber and instilled with amoebae in 20 μl of fresh culture medium. Group 2 received trophozoites that were

pretreated with anti-GH antibodies (30 µg/ml) for 20 min. Group 3, noninfected mice, animals were inoculated only with culture medium. Mouse mortality was determined using survival curves, and the significance was calculated using the log-rank test [32].

Results

• Secretory products of *N. fowleri* contain mucinolytic proteins

To detect proteolytic activity in the secretory products of *N. fowleri*, supernatants from 12 h (from amoebae with 99% viability) were analyzed in gelatin co-polymerized gel (gelatin-zymogram). Clear proteolytic bands at 94, 75, 53 and 40 kDa were obtained when the gels were activated at pH 5 (**Figure 1A**, lane 1). In the case of proteases activated with buffer at pH 7, proteolytic bands were observed at 148, 94, 75 and 53 kDa, and activity at 148, 110, 94 and 53 kDa was observed at pH 9 (**Figure 1A**, lanes 2–3). However, no degradation bands were observed in zymograms that were co-polymerized with bovine submaxilliar mucin (BSM; BSM–zymogram) at any pH analyzed (data not shown). To further analyze the effects of *N. fowleri*-secreted products on mucin, the supernatants were concentrated by precipitation with ethanol. The precipitated samples (ethanol-treated SPs) allowed us to observe two clear bands of mucinolytic activity, >250 kDa and at 94 kDa, in the BSM–zymogram activated at pH 5 (**Figure 1B**, lane 1), whereas the same bands (>250 and 94 kDa), and an additional 53-kDa band were observed in BSM–zymograms activated at pH 7 (**Figure 1B**, lane 2). The BSM–zymogram activated at pH 9 did not reveal any mucinolytic activity and was used as the experimental control, where only bactocasitone serum-free medium was used (**Figure 1B**, lanes 3 & 4).

• Mucinolytic activities are susceptible to cysteine & serine protease inhibitors

To determine the types of proteases that are present in ethanol-treated SPs, various protease inhibitors were used: pHMB, NEM, E-64 and IAA (cysteine protease inhibitors). These inhibitors showed different levels of inhibition compared with the BSM–zymogram without inhibitors (**Figure 2A**, lane 1). The best cysteine-protease inhibitor tested was pHMB,

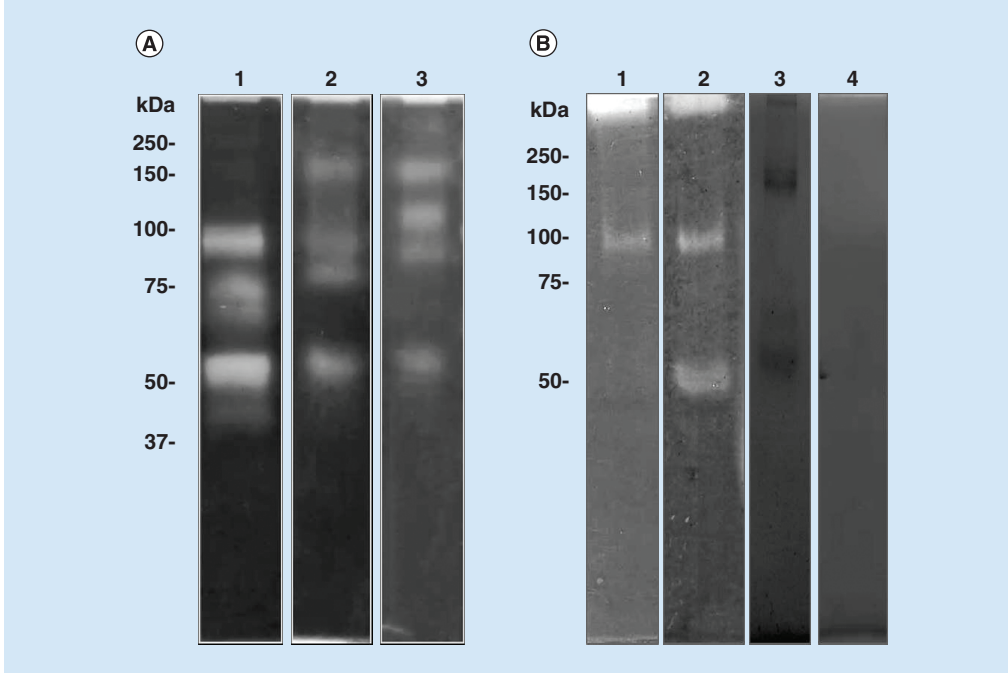

Figure 1. Proteolytic and mucinolytic patterns evaluated at various pH values.
(A) Gelatin–zymogram showing proteolytic bands from secretory products at pH 5, 7, and 9; lanes 1–3, respectively. **(B)** Bovine submaxillary mucin–zymogram showing mucinolytic activities of ethanol-treated secretory products at pH 5 (lane 1: >250 and 94 kDa) and pH 7 (lane 2: >250, 94 and 53 kDa). Mucinolytic activities were not evident at pH 9 (lane 3). Bactocasitone medium at pH 7 (100 mM Trizma and 2 mM $CaCl_2$) was used as a negative control (lane 4). All activities were evaluated at 37°C.

which was able to show total inhibition of the 94- and 53-kDa bands (**Figure 2A**, lane 2); E-64 (**Figure 2A**, lane 3), NEM and IAA (**Figure 2A**, lanes 4 & 5) caused slight inhibition of 94-kDa activity. In contrast, when serine-protease inhibitors were used, the protease activity of the clear band above 250 kDa was completely inhibited by PMSF (**Figure 2A**, lane 6). Aprotinin, the other serine-protease inhibitor, caused similar levels of inhibition of the >250 kDa band, but interestingly, a new clear band of approximately 80 kDa was observed (**Figure 2A**, lane 7). Finally, a specific inhibitor of metalloproteases, 1,10-phenanthroline, did not have an inhibitory effect on these activities (**Figure 2A**, lane 8). To compare these inhibition effects on mucinolytic activities (>250, 94 and 53 kDa), densitometric analyses were performed. The activity at 250 kDa was inhibited mainly by PMSF and aprotinin and partially by pHMB. The activity at 94 kDa was completely inhibited by pHMB and partially inhibited in the following order: E-64, NEM and IAA. Finally, the activity at 53 kDa was completely inhibited by pHMB and partially inhibited at the same magnitude by E-64, NEM and IAA **(Figure 2B)**. All the zymograms were activated at pH 7. These activities were analyzed in three independent assays that showed similar results (*$p < 0.05$).

• Induction of secreted mucinases by BSM

To determine whether these mucinolytic activities were inducible, trophozoites were preincubated with BSM at different times and SPs were recovered and treated with ethanol and analyzed in BSM–zymograms. The results showed that preincubation of amoebae with BSM allowed the induction of only the 94-kDa mucinase of

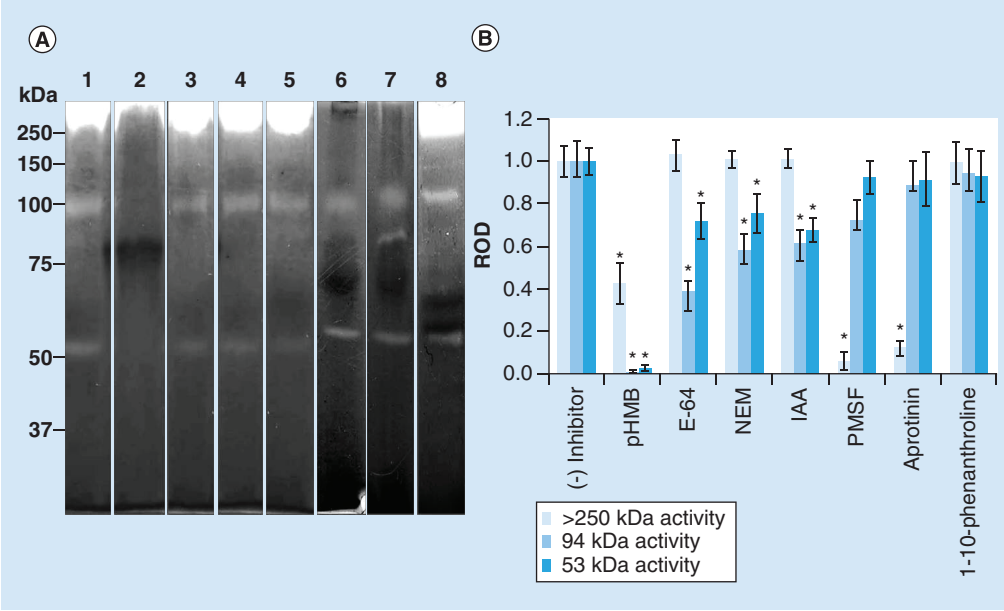

Figure 2. Cysteine and serine protease inhibitors decrease mucinolytic activities. (A) Ethanol-treated secretory products were incubated with protease inhibitors and evaluated in bovine submaxillary mucin–zymograms as follows: ethanol-treated secretory products without inhibitor (lane 1), or with 10 mM pHMB (lane 2), 10 μM E-64 (lane 3), 5 mM NEM (lane 4), 5 μM IAA (lane 5), 5 mM PMSF (lane 6), aprotinin (lane 7), or 10 mM 1,10-phenanthroline (lane 8). All the zymograms were activated at pH 7, the results correspond a one gel with several lanes. **(B)** Densitometric analyses of >250-kDa (white bars), 94-kDa (black bars) and 53-kDa (gray bars) protein activities using ImageJ software, graphed by GraphPad Prism and expressed as ROD values. Statistical analysis was performed by two-way ANOVA comparing the degradation without inhibitors. Bars display the mean ± SE of three independent assays.
*$p < 0.05$.
E-64: 1-{*N*-[(L-3-trans-carboxyoxirane-2-carbonyl)-L-leucyl]amino}-4-guanidinobutane;
IAA: Iodoacetamide; NEM: N-ethylmaleimide; pHMB: p-hydroxymercuribenzoate; PMSF: Phenylmethyl sulfonyl fluoride; ROD: Relative optical density.

N. fowleri, which increased in a time-dependent manner (from 1 to 12 h; **Figure 3A**, lanes 1–4). For comparison purposes, trophozoites without preincubation with BSM (noninducible) were also analyzed. These zymograms detected activity at >250-, 94- and 53-kDa after 6 and 12 h of incubation (**Figure 3B**, lanes 7–8). Densitometric analysis of the 94-kDa mucinase in inducible and noninducible conditions showed that this mucinase is clearly inducible after 1, 3 and 6 h (*$p < 0.05$). At 12 h, both conditions, inducible and noninducible, reached activity that was similar to the control activity of the 94-kDa protein **(Figure 3C)**.

• Identification of mucinolytic proteins by mass spectrometry

Because the 94-kDa protein with mucinolytic activity was inducible and increased after interaction with mucin, we sought to identity this mucinase using mass spectrometry. Bands of 94 kDa from the BSM–zymogram and the SDS-PAGE gel were analyzed by mass spectrometry. Both analyses showed that this band contained 28 different fingerprint proteins identified in the *N. gruberi* genome that could be classified into six different groups of proteins according to cellular functions including 41% metabolic, 30% proteases and hydrolases, 11% undetermined, 7% heat-shock proteins, 7% signaling and 4% synthesis. From these fingerprints, the GH with a molecular weight of 95.3 kDa was used for further experiments, as this protein had the highest coverage (21.55).

• Activity of glycosidases of the 94-kDa protein of *N. fowleri*

The 94-kDa mucinase was partially purified from supernatants of *N. fowleri*. Ethanol-treated SPs were separated by chromatography in an anion-exchange column. All eluted fractions from the column were collected and analyzed using SDS-PAGE and BSM–zymograms. The results revealed lower cationic properties for the 94-kDa protein, as this fraction with mucinolytic activity eluted at 300 mM NaCl (MEF). SDS-PAGE 10% results showed differences in the

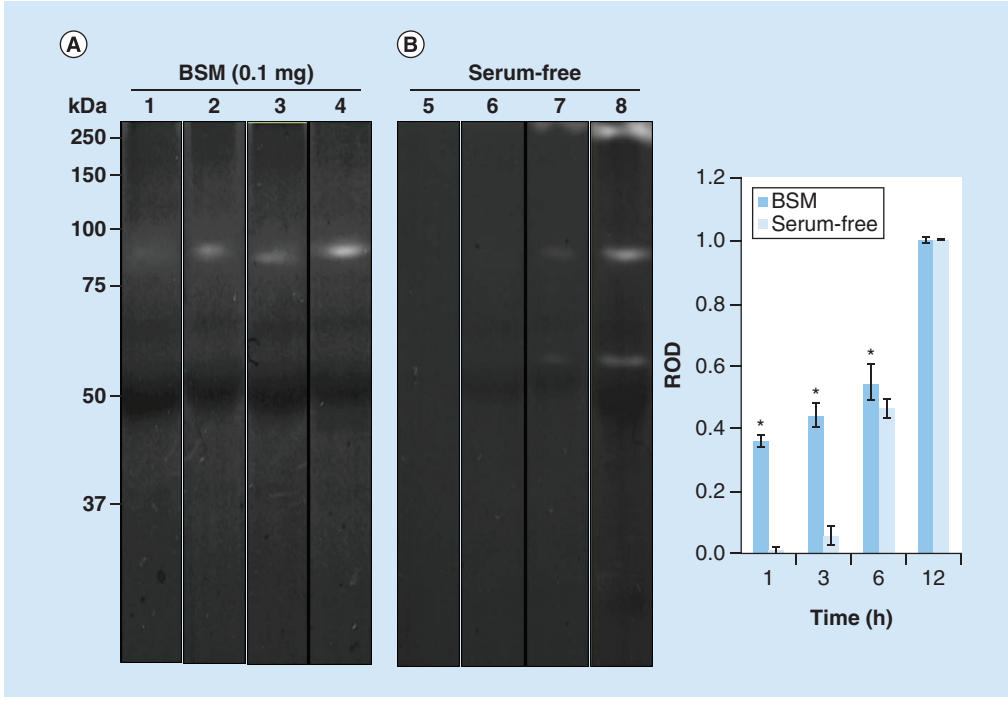

Figure 3. Secretion of an inducible *Naegleria fowleri* mucinase of 94 kDa using BSM. (A) *N. fowleri* trophozoites were exposed to 0.1 mg/ml BSM for 1, 3, 6 and 12 h, and the ethanol-treated secretory products from *N. fowleri* were tested in a BSM–zymogram. Activity at 94 kDa was detected at all times evaluated (lanes 1–4). SPs from nonstimulated trophozoites revealed bands of >250, 94 and 53 kDa, but only at 6 and 12 h (lanes 7 & 8). **(B)** Statistical analysis was performed by two-way ANOVA comparing degradation without inhibitors. All bars display the mean ± SE of three independent assays.
*$p < 0.05$.
BSM: Bovine submaxillary mucin; ROD: Relative optical density.

protein profile of ethanol-treated SPs and MEF (**Figure 4A**, lanes 2 & 3). Moreover, the mucinolytic profiles of ethanol-treated SPs showed the previously described activities at >250-, 94- and 53-kDa (**Figure 4A**, lane 4), whereas the BSM–zymogram of MEF only contained the 94-kDa activity (**Figure 4A**, lane 5). However, the >250-kDa activity eluted with 400 and 500 mM NaCl (data not shown) and the 53-kDa activity was not found in any eluted fraction (data not shown).

According to the mass spectrometry data, this 94-kDa protein is a glycosidase, and therefore, we decided to evaluate the activity of this enzyme using various carbohydrates coupled to the chromogenic 4-nitrophenyl-group substrate. Our results showed that both ethanol-treated

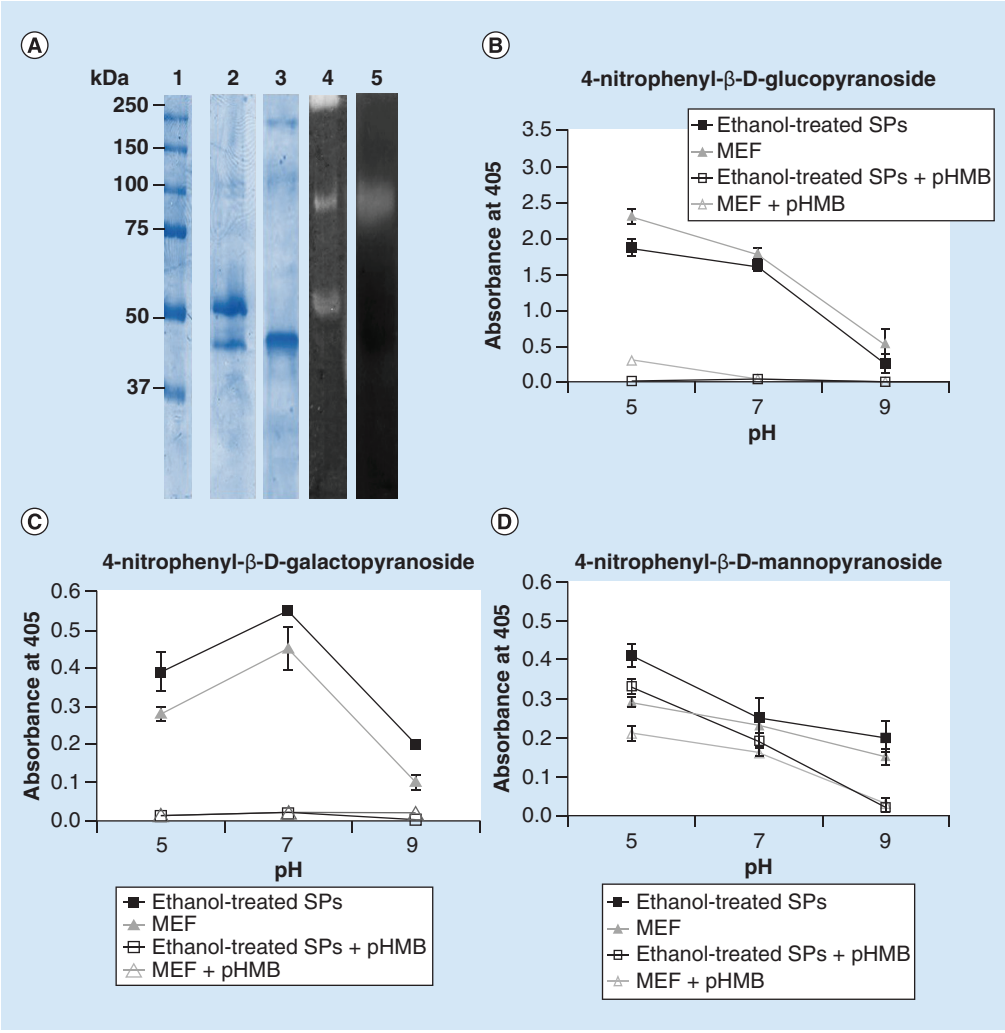

Figure 4. Degradation of glycosidic substrates by glycosidases from *Naegleria fowleri*. (A) SDS-PAGE 10%: molecular weight marker (lane 1), ethanol-treated SPs (lane 2) and MEF (lane 3) samples. BSM–zymogram of ethanol-treated SPs (lane 3) and MEF (lane 4) samples. **(B)** Activity of ethanol-treated SPs (solid squares) and MEF (solid triangles) on β-galactopyranoside. **(C)** Activity of ethanol-treated SPs (solid squares) and MEF (solid triangles) on β-glucopyranoside. **(D)** Activity of ethanol-treated SPs (solid squares) and MEF (solid triangles) on β-mannopyranoside. For each substrate, ethanol-treated SPs and MEF were also pretreated with 10 mM pHMB (empty squares and empty triangles, respectively). Enzymatic activities were analyzed at various pH values and determined spectrophotometrically at 405 nm. Statistical analysis two-way ANOVA was performed, and the data are reported as the means ± SEM of three independent experiments.
*$p < 0.05$.
MEF: Mucinase-enriched fraction; pHMB: p-hydroxymercuribenzoate; SP: Secretory product.

SPs and the MEF from *N. fowleri* were able to hydrolyze β-D-glucopyranoside at pH 5 and 7 but not at pH 9 **(Figure 4B)**. To a lesser extent, both ethanol-treated SPs and MEF also hydrolyzed 4-nitrophenyl β-D-galactopyranoside at pH 5 and mainly at pH 7 **(Figure 4C)**, while the hydrolysis of β-D-mannopyranoside occurred mainly at pH 5 but also at pH 7 **(Figure 4D)**. Remarkably, the inhibitor pHMB (at 10 mM) was able to completely inhibit the hydrolysis activity against β-D-glucopyranoside **(Figure 4B)** and 4-nitrophenyl-β-D-galactopyranoside at all evaluated pH values **(Figure 4C)**. However, this inhibitor caused less inhibition on β-D-mannopyranoside (*$p < 0.05$; **Figure 4D**).

• GH is detected in SPs & trophozoites from *N. fowleri*

To obtain antibodies against GH, a synthetic peptide was designed to be used as an antigen

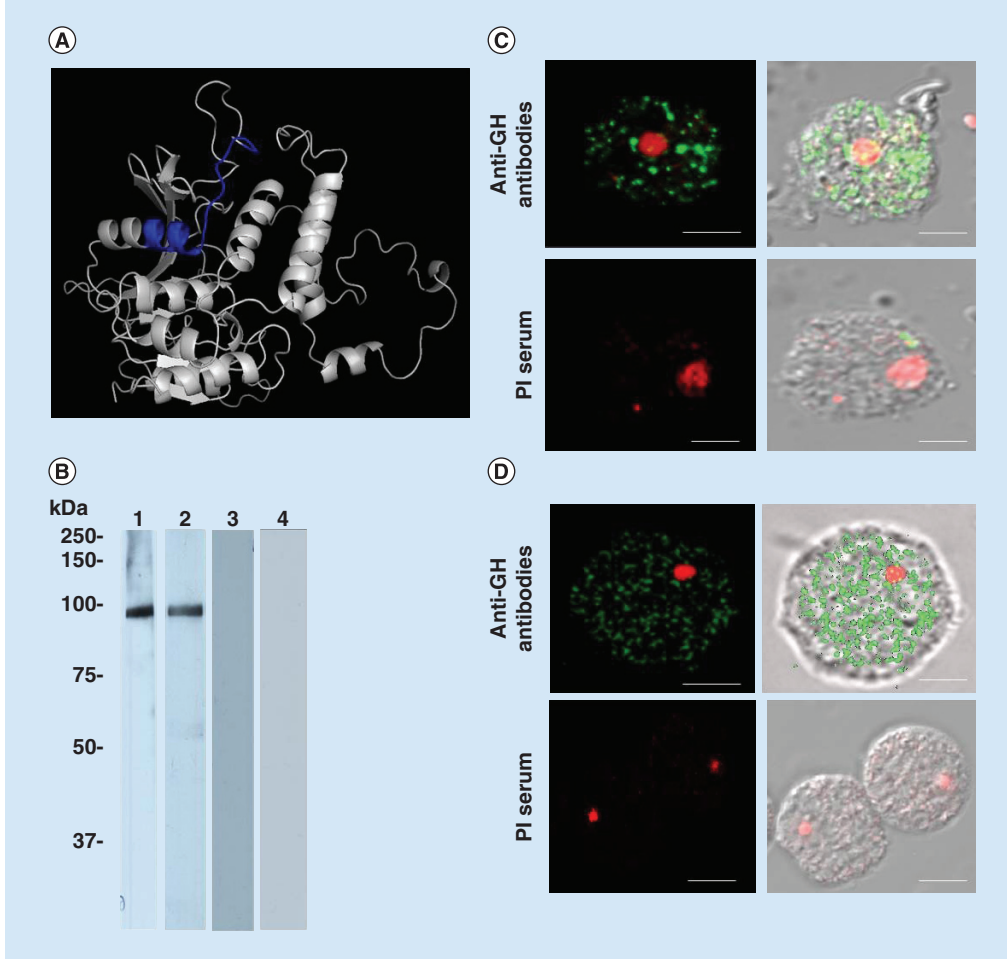

Figure 5. Identification of Nf-GH in *Naegleria fowleri* trophozoites using antibodies against glycoside hydrolase. (A) 3D prediction of GH showing the selected peptide sequence (blue) to obtain the specific GH antibodies (anti-GH). **(B)** Detection of Nf-GH in ethanol-treated secretory products and mucinase-enriched fraction. Wb assays: secretory products (lane 1) and mucinase-enriched fraction (lane 2) samples; a specific band at 94 kDa was detected by the anti-GH antibodies. The rabbit PI serum was tested in secretory products and mucinase-enriched fraction (lanes 3 & 4) as experimental controls **(C)** Localization of Nf-GH in *N. fowleri* trophozoites under nonpermeabilized conditions. **(D)** Localization of Nf-GH in *N. fowleri* trophozoites under permeabilized conditions; the amoebae were permeabilized with 0.2% Triton X-100. Anti-GH recognition was detected using a secondary FITC-conjugated antibody, whereas nuclei were labeled with propidium iodide. The PI serum was used as a control. Images were obtained by confocal microscopy (Carl Zeiss, LMS 700) at 60×, scale bar, 10 μm.
GH: Glycoside hydrolase; Nf-GH: GH of *Naegleria fowleri*; PI: Preimmune.

to immunize rabbits. *In silico* analysis of the GH (access number: 284096877) obtained from the NCBI database revealed that this hydrolase contains the GH31 domain, which is capable of processing the N-linked oligosaccharides. This prediction correlated with our previously described findings regarding the activity of the MEF on these types of substrate. In addition, the 3D prediction performed by the Phyre[2] software, using as a template α- and β-hydrolases (d2pI5a1) from *Leptospira interrogans* and the sequence of GH from *N. gruberi*, allowed us to obtain the predicted 3D structure of GH with 32% coverage (342 residues) and 99.6% confidence. Moreover, the 3D analysis revealed that the catalytic residues are localized at the G (678), H (951) and D (922) amino acid residues. By using three software packages, as indicated in the 'Materials & Methods' section, a sequence close to the active site was chosen based on hydrophobicity, immunogenicity, flexibility, accessibility, turn and polarity. This antigenic peptide of 18 amino acids contained residues 640–658 of GH **(Figure 5A)**. After immunization of rabbits with the synthetic peptide coupled to KLH, the antibody titers were evaluated by the ELISA method, which reached an end-point dilution of 1:64,000 using ethanol-treated SPs as the antigen (data not shown). Remarkably, antibodies recognized the 94-kDa band in ethanol-treated SPs and MEF from *N. fowleri* **(Figure 5B**, lanes 1 & 2), whereas the PI serum did not show any recognition band (**Figure 5B**, lanes 3 & 4) in Wb assays. Thus, we designated this protein the GH of *N. fowleri* (Nf-GH). Additionally, by confocal microscopy, the GH was detected in nonpermeabilized **(Figure 5C)** and permeabilized **(Figure 5D)** amoebae in the cytoplasm and also at the cytoplasmic membrane.

• Antibodies against GH prevent the cytopathic effect induced by *N. fowleri* trophozoites on mucoepithelial cells

Antibodies against GH were added simultaneously with trophozoites of *N. fowleri* to mucoepithelial cell monolayers and incubated for 1, 3 and 6 h. The cytopathic effect was analyzed by fluorescence. The data showed that anti-GH antibodies drastically reduced the cell damage of the NCI-H292 cell monolayers caused by *N. fowleri* trophozoites from 1 to 6 h of incubation **(Figure 6A)** compared with cells incubated with *N. fowleri* in the absence of anti-GH antibodies **(Figure 6A)**. The mean fluorescence intensity of the images confirmed the protective effect of the anti-GH antibody against NCI-H292 cell damage induced by *N. fowleri*. Untreated cells incubated with anti-GH antibodies were used as a negative control, whereas cells treated with Triton X-100 were used as a positive control and showed the highest mean fluorescence intensity (*$p < 0.001$; **Figure 6A & B**).

• Human MUC5AC degradation is inhibited by anti-GH antibodies

To determine whether the MUC5AC mucin is the target of Nf-GH, NCI-H292 cells were induced to secrete this type of mucin by incubation with PMA. These secreted glycoproteins were used as a substrate in zymogram gels, as mentioned in the 'Materials & Methods' section. Using 5% SDS-PAGE, the results showed a predominant band of approximately 250 kDa (likely not resolved; **Figure 7A**, lane 2). Moreover, the band near 250 kDa was recognized by the anti-Mucin 5AC antibody in Wb assays (**Figure 7A**, lane 3). To corroborate the MUC5AC mucin degradation, the ethanol-treated SP samples were separated in zymograms co-polymerized with mucins from NCI-H292 cells. We detected three clear bands of mucinolytic activity at >250 kDa, 94 kDa and 53 kDa (data not shown), similar to those detected in BSM–zymograms.

Moreover, the MEF was loaded in the zymogram containing the secreted mucin, and a clear band was detected near 94 kDa (**Figure 7B**, lane 1). Interestingly, this activity was partially inhibited by anti-GH antibodies before loading onto the zymogram (**Figure 7B**, lane 2). Furthermore, the mucinolytic activity was completely inhibited with 10-mM pHMB (**Figure 7B**, lane 3). These results were confirmed by densitometric analysis from three independent assays (*$p < 0.05$; **Figure 7C**).

To demonstrate that MUC5AC is a target of Nf-GH, secreted mucins were incubated with the MEF or MEF preincubated with pHMB and MEF with anti-GH antibodies. As a positive-degradation control, the secreted mucins were treated with PK, and the negative control was the untreated secreted mucins. The ethanol-treated SP from *N. fowleri* without secreted mucins were also used as a negative control. With the aim to corroborate the loaded protein, the nitrocellulose membrane was stained with Ponceu's solution **(Figure 7D)**. Mucinolytic activities were analyzed by dot-blot using antibodies against MUC5AC. As expected, PK was able to

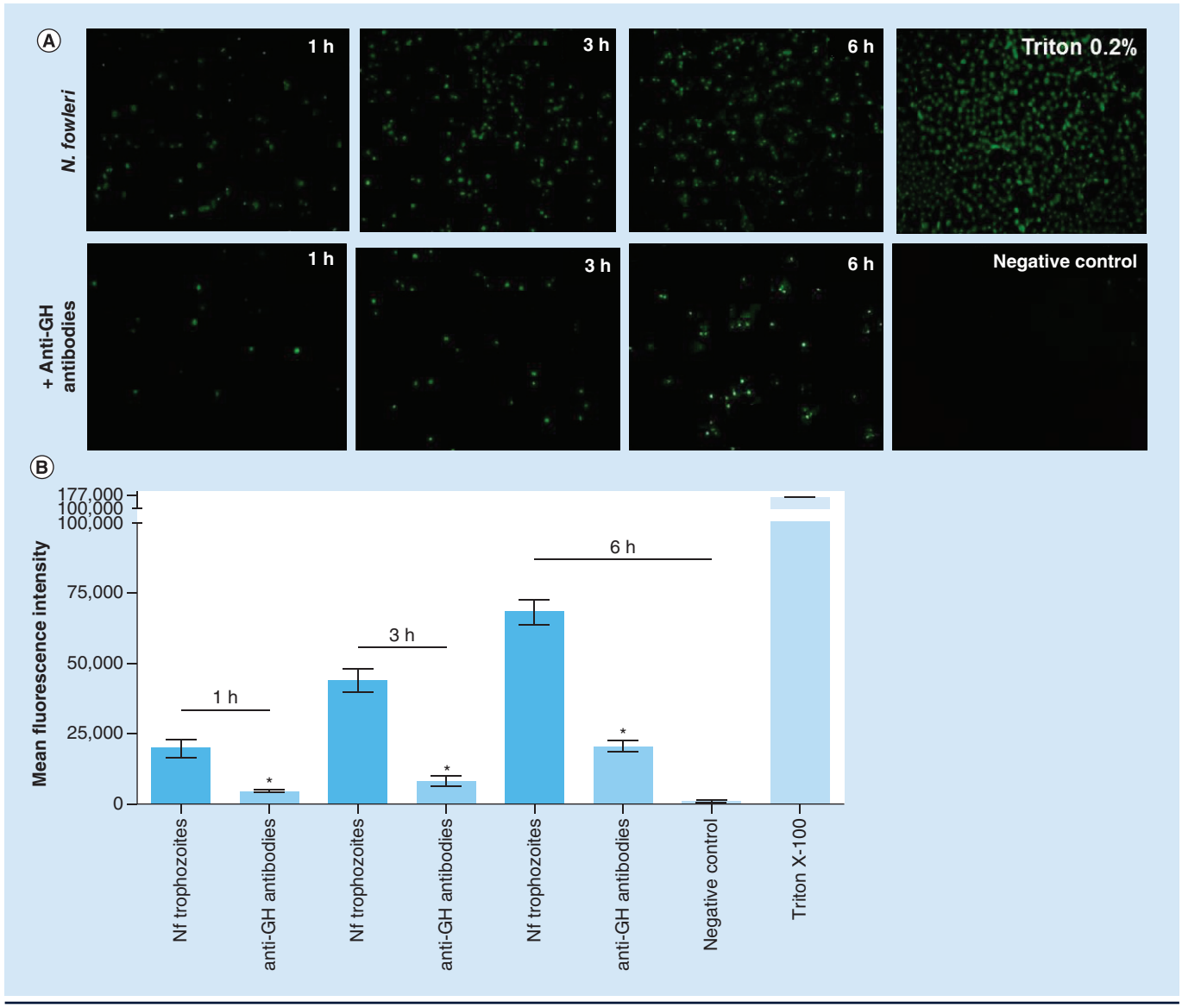

Figure 6. Protective effect of anti-GH antibodies on NCI-H292 cell death induced by *Naegleria fowleri* trophozoites. (A) *N. fowleri* trophozoites co-incubated with NCI-H292 during 1, 3 and 6 h in the absence or presence of anti-GH antibodies (1.5 μg/ml). Anti-GH antibodies prevent cell death even at 6 h. NCI-H292 cells without trophozoites were used as a negative control, while cells treated with 0.2% Triton X-100 were used as a positive control. Cell viability was evaluated using SYTOX green, which marks dead cells in green. Images were obtained with a fluorescent inverted Nikon microscope (eclipse Ti-U) at 20×. **(B)** Quantification of the fluorescence intensity of labeled nuclei using ImageJ software. All bars display the mean ± SE of three independent experiments.
*$p < 0.001$.
GH: Glycoside hydrolase; Nf: *Naegleria fowleri*.

degrade MUC5AC, as detected by the absence of a signal from the anti-Mucin 5AC antibody as compared with the strong detection of MUC5AC in the secreted mucins. Interestingly, MEF was able to degrade MUC5AC; this degradation was inhibited by pHMB and anti-GH antibodies (**Figure 7D**). Densitometry analyses of three independent experiments confirmed the MUC5AC degradation by MEF and the prevention of this activity by pHMB and anti-GH antibodies (*$p < 0.05$; **Figure 7E**).

• Anti-GH antibodies delay mouse mortality in an experimental PAM infection

To understand the role of Nf-GH during *in vivo* infection by *N. fowleri*, anti-GH antibodies were used to prevent the mouse mortality induced by *N. fowleri* trophozoites. To perform experimental

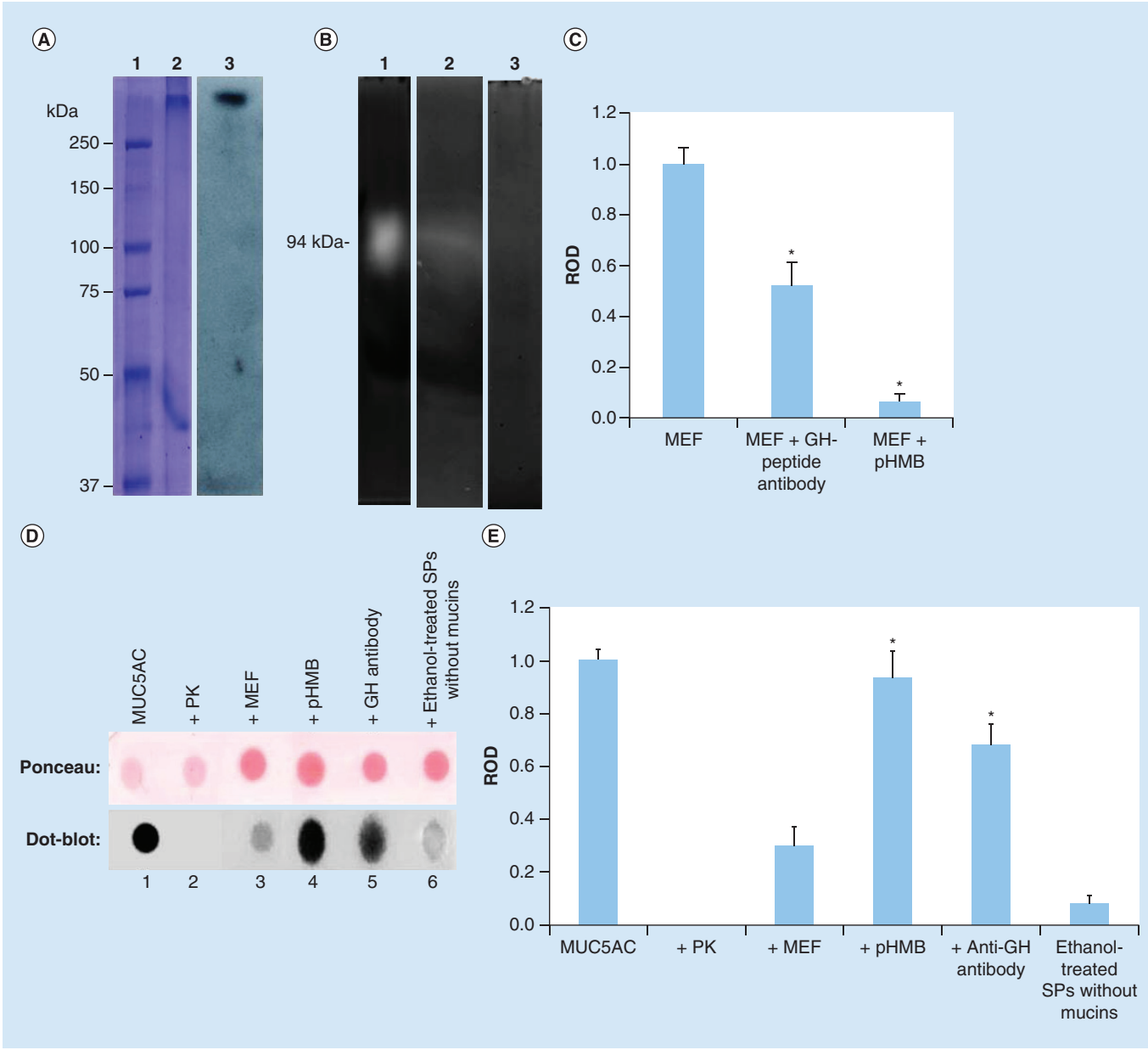

Figure 7. *Naegleria fowleri* GH causes MUC5AC degradation. (A) Detection of MUC5AC in secreted mucin from NCI-H292 cells. SDS-PAGE: molecular weight marker (lane 1), secreted mucin from NCI-H292 cells (lane 2), two evident bands at >250 kDa and 40 kDa are shown. Western blot: Detection of the >250-kDa protein of secreted mucin from NCI-H292 cells using the anti-MUC5AC antibody (lane 3). **(B)** Zymogram copolymerized with secreted mucins from NCI-H292 cells was used as substrate. MEF loaded alone (lane 1), MEF preincubated with anti-GH antibodies (lane 2) or MEF preincubated with pHMB inhibitor (lane 3); gels were activated at pH 7 and 37°C. Mucinolytic activity at approximately 94 kDa by *Naegleria fowleri* GH was observed (lane 1). **(C)** Densitometric analysis of panel A was performed using ImageJ and GraphPad Prism software; *$p < 0.05$. **(D)** Detection of MUC5AC degradation by MEF by dot-blot (dot 1), secreted mucins from mucoepithelial cells without treatment; (dot 2) secreted mucins treated with PK, (dot 3) secreted mucins treated with 94-kDa fraction, (dot 4) secreted mucins treated with *Naegleria fowleri* GH preincubated with pHMB, (dot 5) secreted mucins treated with MEF preincubated with anti-GH antibodies, (dot 6) secretory products without secreted mucins, used as a negative control. All dot-blots were developed using antibodies against the MUC5AC mucin. The load protein was stained with Ponceu's solution. **(E)** Densitometric analysis of MUC5AC degradation of the assays shown in panel D was performed using ImageJ software. Bars display the mean ± SE of three independent assays. *$p < 0.05$.

GH: Glycoside hydrolase; MEF: Mucinase-enriched fraction; pHMB: p-hydroxymercuribenzoate; PK: Proteinase K; ROD: Relative optical density.

PAM, groups of six animals were instilled with 12×10^4 amoebae. After infection, a curve of the log-rank test was constructed to compare the survival of all animals evaluated. The infected mice (group 1) all died at 7 days postinfection, while the noninfected group (group 3) survived until the end of the experiment (100% survival). Interestingly, when the trophozoites were preincubated with anti-GH antibodies (group 2), animals showed a delayed mortality, with 50% survival at 10 days and the remaining mice died (50%) at 17 days postinstillation (*$p < 0.001$; **Figure 8A**).

Discussion

Mucus serves as a physical barrier that protects against foreign agents including toxins, pathogens and environmental particles and is largely composed of mucin networks secreted by goblet cells and seromucinous glands [33]. The composition of nasal mucus includes water, lysozyme, lactoferrin, complement, secretory IgA, IgM and mucins (glycoproteins). Glycoproteins comprise

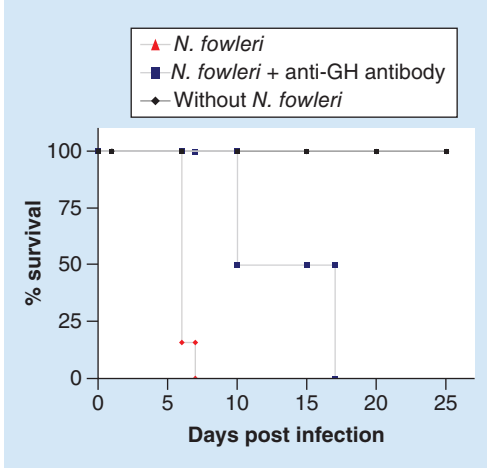

Figure 8. Mouse mortality by primary amoebic meningoencephalitis was delayed using anti-GH antibodies. Mouse mortality was determined in animals instilled with amoebae (12×10^4; triangles) and amoebae preincubated with anti-GH antibodies (30 μg/ml) (squares). Noninfected animals were used as negative controls (diamonds). Infected mice with trophozoites showed mortality 7 days postinfection, while mouse mortality was delayed using anti-GH antibodies for 17 days. The noninfected group survived the entire experiment. Survival curves were analyzed by the log rank test using GraphPad Prism (n = 6, per group).
*$p < 0.001$.
GH: Glycoside hydrolase.

80% of the dry weight of mucus. Mucins are up to 5-μm long and consist of random coils of carbohydrate chains attached to a protein core via O-glycoside linkages. However, the NH_2 and COO^- regions are poorly glycosylated [34]. Changes in the rheological properties of mucus alter the functions of the molecule, which include lubrication, serving as a selective barrier, and protecting against infection [35–37]. For example, a decrease in the viscosity of vaginal mucus has been correlated with bacterial vaginitis, and this change increases the risk of HIV and other infections [37,38]. The basal secretion rates of mucus in the nasal epithelium have been reported to be approximately 15.7 ± 6.0 pl/min^{-1} per $gland^{-1}$; however, mucus secretion can be modified under various conditions, such as cystic fibrosis, chronic rhinosinusitis or microbial infection [39,40]. It is well known that pathogenic microorganisms depend on successful colonization of the host to survive and multiply. Pathogens use several strategies including secretion of proteolytic molecules to evade the host's innate immune response. Indeed, such proteases and enzymes associated with mucus degradation have been reported for bacteria, virus and other parasites [40,41]. Molecules degrading mucus have also been reported in mucin-dwelling protozoans [18].

It is well known that *N. fowleri* enters the nasal cavity and is able to avoid various immune responses, causing acute and fulminant PAM disease in humans [42]. During the first stages of experimental PAM, these microorganisms are surrounded by neutrophils and abundant mucus [11]. However, it has been observed that trophozoites are able to evade this innate response until they reach the central nervous system [10], and this evasion has been correlated with various mechanisms of pathogenicity in *in vitro* systems [6,43–45]. Previously, our group reported a 37-kDa mucinase in the total crude extracts of *N. fowleri* using BSM as a substrate [21], and this finding led us to investigate whether the pathogen is able to release such mucinases and to identify and characterize biochemically the putative proteases.

An ethanol-precipitated strategy and zymogram assays provided information about the total proteins with mucinolytic activity in supernatants from *N. fowleri*; these experimental strategies have proven useful in characterizing proteolytic activities in bacteria and free-living amoebae [9,46,47]. Using this approach, we could

observe, for the first time, three evident mucinolytic activities at pH 5 and 7 in ethanol-treated SPs of *N. fowleri* using BSM-copolymerized zymogram as a substrate. The pH values evaluated were consistent with those in different regions of the human nasal cavity [25]. It is also known that pH plays an important role in the activity of proteolytic proteins in *N. fowleri* and other microorganisms [7,48]. The mucinolytic activities were compared with a nonspecific substrate (porcine gelatin 0.1%), and various patterns of activity were observed, suggesting that secreted proteases have substrate specificity.

Several reports have shown that the main proteases present in *N. fowleri* are cysteine proteases; some serine proteases have been experimentally reported in *Naegleria* species, and metalloproteases are also present in a smaller proportion [6–8,49]. According to these data, we found that cysteine and serine protease inhibitors primarily decreased BSM degradation. While cysteine proteases show susceptibility to the E-64 cysteine protease inhibitor in *N. fowleri* [7,49], this inhibitor mainly affects CA proteases [50,51]; in contrast, protease activities were completely inhibited by pHMB. Unlike E-64, pHMB attaches to cysteine and binds to thiol groups; both thiols and cysteine residues are essential for the protease activity [49,52]. Moreover, the pHMB inhibitor is also able to affect the activity of glycosidases. It has been demonstrated in *Lactobacillus plantarum*, in *Neocallimastix frontalis* and in the fungus *Trichoderma* that pHMB participates in the inhibition of α-L-rhamnosidases and β-glucosidases [52–55]. In contrast, the >250-kDa protein activity was abolished in the presence of PMSF and aprotinin, suggesting that this fraction contains serine proteases. These results strongly suggest that secreted proteins contain more than one type of molecules involved in mucin degradation.

To invade the epithelium, *N. fowleri* must produce specific mucinases to degrade specific mucins in the microenvironment of the invasion site. In fact, in the case of cysteine proteases secreted by *E. histolytica*, it has been found that the secretion of these cysteine proteases is enhanced during interaction with porcine stomach mucin, suggesting that the specific composition of mucins may be important in influencing the *Entamoeba* phenotype [56]. This may occur during invasion by *N. fowleri*. Indeed, here we show that three mucinolytic activities were detected; however, the only protease with mucin-inducible activity was a 94-kDa mucinase. This result correlated with the previous reports using the mouse model, where the mucus production appears at 1 h postinstillation, so the induction of a mucinase is early as the infection occurs [10,11]. It is probably that the stress condition (serum-free) also stimulates the activity of proteases secretion. Therefore, we focused on the partial purification and identification of this 94-kDa protein. Interestingly, even though the 94-kDa mucinase is slightly cationic, it could be separated in a high-Q-cartridge column; the 94-kDa mucinase showed rapid elution with a lower NaCl concentration, and >250-kDa activity was eluted at a higher concentration of NaCl. Surprisingly, the 53-kDa activity was not eluted from this column in any fraction; it is noteworthy that this 53-kDa activity was also lost when the supernatants were precipitated with ammonium sulfate (data not shown). These data suggest that the 53-kDa band could be a degradation subproduct of a larger protein, possibly from the >250-kDa band. A similar strategy of proteolytic protein purification by exchange chromatography using a mono-Q anion-exchange column was previously reported for *N. fowleri*, though the authors reported proteases at approximately 60 and 30 kDa, as identified in gelatin zymograms [6,57]. Furthermore, mass protein identification by spectrometric analysis of the ethanol-treated SP activity and Coomassie band in one dimension revealed the presence of GH activity at 94 kDa. A fingerprint of the peptides obtained from this protein was assessed using the nonpathogenic *N. gruberi* genome [58]. In addition, we evaluated the SP of *N. gruberi* using BSM–zymograms. Our results showed a 94-kDa activity, so it is possible that this amoeba releases glycosidases in the nature that may be acting in the biofilms that are rich in polysaccharides (data not shown).

The role of proteases and glycosidases in mucin degradation has been reported in *E. histolytica*. Specifically, cysteine proteases, sialidases, α-glucosidase and β-N-acetylhexosaminase have been associated with disruption of the mucin polymeric network [16,17,59]. It has also been shown that the *Fasciola hepatica* supernatants contain a glycosidase that degrades *in vitro* ovine mucin [60]. Thus, our data strongly suggest that a glycosidase released by *N. fowleri* could be participating in mucin degradation. Therefore, we decide to demonstrate the role of GH

in *N. fowleri* because mucin composition is mainly constituted by carbohydrate moieties.

Moreover, in the mid-1980s, several glycosidase activities were reported in the total crude extracts of *N. fowleri*, including β-D-glucosidase, β-D-galactosidase, α-D-glucosidase, β-fucosidase, α-mannosidase and arylsulfatase A [57,61,62]. However, the secretion and role of glycosidases had not been demonstrated until now. Our results show that the MEF of *N. fowleri* can cleave the glycosidic bonds of specific substrates; moreover, these glycosidic activities were inhibited by pHMB [52,53]. The *O*-glycan chains in mucins are synthesized by specific glycosyltransferases that transfer *N*-acetylgalactosamine to Ser or Thr residues and are elongated by the addition of galactose, *N*-acetylglucosamine, fucose, *N*-acetylneuraminic acid and sulfate linkages [63]. In addition, C-mannose residues have been identified in MUC5AC and MUC5B mucin linkages to tryptophan residues [64]; these glycan linkages are also present in the BSM composition [65–67]. Therefore, in our study, we used these types of glycans to demonstrate the activity of GH in *N. fowleri*. With these results we found that SPs and MEF contained a GH that can degrade specific carbohydrates, therefore it is not a protease.

To demonstrate the hypothesis that during *N. fowleri* invasion, the amoeba release hydrolases that alter mucus rheology, we designed a synthetic peptide to generate specific polyclonal antibodies against GH from *N. fowleri*. These antibodies detected a protein of 94 kDa both in ethanol-treated SP and the MEF (Nf-GH). The Nf-GH protein was localized to the cytoplasm and the plasma membrane. More studies are needed to elucidate the secretion pathway of GH in *N. fowleri* trophozoites.

The role of Nf-GH as a mechanism of pathogenicity was supported by the inhibitory effects of anti-GH antibodies on the cytopathic effect induced by trophozoites on mucoepithelial cells. This inhibition event could be related to the high agglutination capacity of the anti-GH antibody in the trophozoites. The agglutination of the amoebae by the antibodies was detected at 1.5 μg/ml (data not shown), a lower concentration than the human basal concentrations of IgG and IgM in the serum, which have been reported to be 1.75 mg/ml and 30.22 mg/ml, respectively [68,69]. Furthermore, anti-GH antibody also diminished human MUC5AC mucin degradation induced by the MEF of *N. fowleri*. Regarding the 75% GH inhibition in MUC5AC mucin degradation, we cannot rule out the role of other proteases in mucin degradation [6,8,9]. Currently, we are working with a dipeptidyl aminopeptidase that acts as a protease; therefore, it is possible that GH works together with other proteases.

Because the anti-GH antibody clearly recognized Nf-GH protein, this antibody is able to inhibit the degradation of MUC5AC mucin and prevent the cytopathic effect of the mucoepithelial cells by *N. fowleri* trophozoites; a relevant study was to verify if this antibody was able to prevent or delay the PAM in mice. These experiments clearly showed the relevance of Nf-GH in the infection, as the antibodies against the GH were able to retard mouse mortality; in addition, the eventual death of the animals could be due to the ability of *N. fowleri* to internalize and degrade antibodies [70].

Our results strongly suggest that released glycosidases cause degradation of MUC5AC mucin and thus alter mucus rheology to allow the migration of *N. fowleri* to the brain. In conclusion, it is essential to consider the mucinolytic activities secreted by *N. fowleri* in the development of new tools for the diagnosis and treatment of *N. fowleri* infection.

Acknowledgments

The authors would like to thank ER Castro, AC Mejía, and OB García for their technical assistance in the sample processing for LC-MALDI-MS/MS. We appreciate A Silva-Olivares for her assistance with the amoeba cultures.

Financial & competing interests disclosure

This work was supported by CONACyT grant number 237523. The authors have no other relevant affiliations or financial involvement with any organization or entity with a financial interest in or financial conflict with the subject matter or materials discussed in the manuscript apart from those disclosed.

English language assistance by American Journal Experts (AJE) was utilized in the production of this manuscript.

Ethical conduct of research

The authors state that they have obtained appropriate institutional review board approval or have followed the principles outlined in the Declaration of Helsinki for all human or animal experimental investigations. In addition, for investigations involving human subjects, informed consent has been obtained from the participants involved.

SUMMARY POINTS

- *Naegleria fowleri* releases factors with mucinolytic activity.
- The 94-kDa factor with activity is inducible by bovine submaxillary mucin and inhibited by p-hydroxymercuribenzoate inhibitor.
- Glycosidases were identified using MALDI-TOF-MS.
- Enzymatic activity in carbohydrates as substrates of secretory products revealed the presence of β-glucosidases, β-glycosidases and β-mannosidases.
- Glycoside hydrolase of 94-kDa was identified in cytoplasm, cellular membrane and secretion products of *N. fowleri*.
- Glycoside hydrolase of *Naegleria fowleri* participates in cellular damage and MUC5AC degradation and has an important role in experimental primary amoebic meningoencephalitis.

References

Papers of special note have been highlighted as:
• of interest; •• of considerable interest

1 Carrasco-Yepez M, Campos-Rodriguez R, Godinez-Victoria M *et al. Naegleria fowleri* glycoconjugates with residues of alpha-D-mannose are involved in adherence of trophozoites to mouse nasal mucosa. *Parasitol. Res.* 112(10), 3615–3625 (2013).

2 Han KL, Lee HJ, Shin MH, Shin HJ, Im KI, Park SJ. The involvement of an integrin-like protein and protein kinase C in amoebic adhesion to fibronectin and amoebic cytotoxicity. *Parasitol. Res.* 94(1), 53–60 (2004).

3 Thong YH, Ferrante A. Migration patterns of pathogenic and nonpathogenic *Naegleria spp*. *Infect. Immun.* 51(1), 177–180 (1986).

4 Sohn HJ, Kim JH, Shin MH, Song KJ, Shin HJ. The *Nf-actin* gene is an important factor for food-cup formation and cytotoxicity of pathogenic *Naegleria fowleri*. *Parasitol. Res.* 106(4), 917–924 (2010).

5 John DT, Cole TB Jr, Marciano-Cabral FM. Sucker-like structures on the pathogenic amoeba *Naegleria fowleri*. *Appl. Environ. Microbiol.* 47(1), 12–14 (1984).

6 Aldape K, Huizinga H, Bouvier J, Mckerrow J. *Naegleria fowleri*: characterization of a secreted histolytic cysteine protease. *Exp. Parasitol.* 78(2), 230–241 (1994).

7 Serrano-Luna J, Cervantes-Sandoval I, Tsutsumi V, Shibayama M. A biochemical comparison of proteases from pathogenic *Naegleria fowleri* and non-pathogenic *Naegleria gruberi*. *J. Eukaryot. Microbiol.* 54(5), 411–417 (2007).

8 Lee J, Kim JH, Sohn HJ *et al.* Novel cathepsin B and cathepsin B-like cysteine protease of *Naegleria fowleri* excretory-secretory proteins and their biochemical properties. *Parasitol. Res.* 113(8), 2765–2776 (2014).

9 Martínez-Castillo M, Ramirez-Rico G, Serrano-Luna J, Shibayama M. Iron-binding protein degradation by cysteine proteases of *Naegleria fowleri*. *Biomed. Res. Int.* 416712 (2015).

10 Rojas-Hernández S, Jarillo-Luna A, Rodriguez-Monroy M, Moreno-Fierros L, Campos-Rodriguez R. Immunohistochemical characterization of the initial stages of *Naegleria fowleri* meningoencephalitis in mice. *Parasitol. Res.* 94(1), 31–36 (2004).

11 Cervantes-Sandoval I, Serrano-Luna J, Garcia-Latorre E, Tsutsumi V, Shibayama M. Characterization of brain inflammation during primary amoebic meningoencephalitis. *Parasitol. Int.* 57(3), 307–313 (2008).

12 Rose MC, Voynow JA. Respiratory tract mucin genes and mucin glycoproteins in health and disease. *Physiol. Rev.* 86(1), 245–278 (2006).

13 Thornton DJ, Rousseau K, Mcguckin MA. Structure and function of the polymeric mucins in airways mucus. *Annu. Rev. Physiol.* 70, 459–486 (2008).

• **Describes the biochemical and functional characteristics of human mucin proteins present in the mucus.**

14 Thornton DJ, Sheehan JK. From mucins to mucus: toward a more coherent understanding of this essential barrier. *Proc. Am. Thorac. Soc.* 1(1), 54–61 (2004).

15 Moncada D, Keller K, Ankri S, Mirelman D, Chadee K. Antisense inhibition of *Entamoeba histolytica* cysteine proteases inhibits colonic mucus degradation. *Gastroenterology* 130(3), 721–730 (2006).

16 Lidell ME, Moncada DM, Chadee K, Hansson GC. *Entamoeba histolytica* cysteine proteases cleave the MUC2 mucin in its C-terminal domain and dissolve the protective colonic mucus gel. *Proc. Natl Acad. Sci. USA* 103(24), 9298–9303 (2006).

17 Moncada D, Keller K, Chadee K. *Entamoeba histolytica* secreted products degrade colonic mucin oligosaccharides. *Infect. Immun.* 73(6), 3790–3793 (2005).

•• **Provides a value information about mucin oligosaccharides degradation by the secreted products.**

18 Connaris S, Greenwell P. Glycosidases in mucin-dwelling protozoans. *Glycoconj. J.* 14(7), 879–882 (1997).

19 Hysmith RM, Franson RC. Degradation of human myelin phospholipids by phospholipase-enriched culture media of pathogenic *Naegleria fowleri*. *Biochim. Biophys. Acta* 712(3), 698–701 (1982).

20 Shibayama M, Serrano-Luna J, Rojas-Hernández S, Campos-Rodriguez R, Tsutsumi V. Interaction of secretory immunoglobulin A antibodies with *Naegleria fowleri* trophozoites and collagen type I. *Can. J. Microbiol.* 49(3), 164–170 (2003).

21 Cervantes-Sandoval I, Serrano-Luna J, Garcia-Latorre E, Tsutsumi V, Shibayama M. Mucins in the host defence against *Naegleria fowleri* and mucinolytic activity as a possible means of evasion. *Microbiology* 154(Pt 12), 3895–3904 (2008).

•• **First report of the mucinolytic activity induced by *Naegleria fowleri* trophozoites.**

22 Cerva L. Amoebic meningoencephalitis: axenic culture of *Naegleria*. *Science* 163(3867), 576 (1969).

23 Shibayama M, Martinez-Castillo M, Silva-Olivares A *et al.* Disruption of MDCK cell tight junctions by the free-living amoeba *Naegleria fowleri*. *Microbiology* 159(Pt 2), 392–401 (2013).

24 Bradford MM. A rapid and sensitive method for the quantitation of microgram quantities of protein utilizing the principle of protein–dye binding. *Anal. Biochem.* 72, 248–254 (1976).

25 Hehar SS, Mason JD, Stephen AB *et al.* Twenty-four-hour ambulatory nasal pH monitoring. *Clin. Otolaryngol. Allied Sci.* 24(1), 24–25 (1999).

26 Schneider CA, Rasband WS, Eliceiri KW. NIH Image to ImageJ: 25 years of image analysis. *Nat. Methods* 9(7), 671–675 (2012).

27 Perkins DN, Pappin DJ, Creasy DM, Cottrell JS. Probability-based protein identification by searching sequence databases using mass spectrometry data. *Electrophoresis* 20(18), 3551–3567 (1999).

28 Systat Version 12. FSS, Inc. San Jose, CA, USA. www.sigmaplot.com

29 Kelley LA, Mezulis S, Yates CM, Wass MN, Sternberg MJ. The Phyre2 web portal for protein modeling, prediction and analysis. *Nat. Protoc.* 10(6), 845–858 (2015).

• **Provides all the tools to perform a 3D prediction in the modeling of proteins.**

30 Saha S, Raghava GP. Prediction of continuous B-cell epitopes in an antigen using recurrent neural network. *Proteins* 65(1), 40–48 (2006).

• **Explains the methodology to design a specific and highly immunogenic peptides to produce antibodies.**

31 Kyte J, Doolittle RF. A simple method for displaying the hydropathic character of a protein. *J. Mol. Biol.* 157(1), 105–132 (1982).

32 Bland JM, Altman DG. The logrank test. *BMJ* 328(7447), 1073 (2004).

33 Gendler SJ, Spicer AP. Epithelial mucin genes. *Annu. Rev. Physiol.* 57, 607–634 (1995).

34 Bansil R, Stanley E, Lamont JT. Mucin biophysics. *Annu. Rev. Physiol.* 57, 635–657 (1995).

35 Tiewcharoen S, Phurttikul W, Rabablert J *et al.* Effect of synthetic antimicrobial peptides on *Naegleria fowleri* trophozoites. *Southeast Asian J. Trop. Med. Public Health* 45(3), 537–546 (2014).

36 Hicks SJ, Theodoropoulos G, Carrington SD, Corfield AP. The role of mucins in host–parasite interactions. Part I-protozoan parasites. *Parasitol. Today* 16(11), 476–481 (2000).

37 Quraishi MS, Jones NS, Mason J. The rheology of nasal mucus: a review. *Clin. Otolaryngol. Allied Sci.* 23(5), 403–413 (1998).

38 Lai SK, Wang YY, Wirtz D, Hanes J. Micro- and macrorheology of mucus. *Adv. Drug Deliv. Rev.* 61(2), 86–100 (2009).

39 Jeong JH, Hwang PH, Cho DY, Joo NS, Wine JJ. Secretion rates of human nasal submucosal glands from patients with chronic rhinosinusitis or cystic fibrosis. *Am. J. Rhinol. Allergy* 29(5), 334–338 (2015).

40 Linden SK, Sutton P, Karlsson NG, Korolik V, Mcguckin MA. Mucins in the mucosal barrier to infection. *Mucosal Immunol.* 1(3), 183–197 (2008).

41 Roberton AM, Wiggins R, Horner PJ *et al.* A novel bacterial mucinase, glycosulfatase, is associated with bacterial vaginosis. *J. Clin. Microbiol.* 43(11), 5504–5508 (2005).

42 Visvesvara GS. Infections with free-living amebae. *Handb. Clin. Neurol.* 114, 153–168 (2013).

43 Herbst R, Ott C, Jacobs T, Marti T, Marciano-Cabral F, Leippe M. Pore-forming polypeptides of the pathogenic protozoon *Naegleria fowleri*. *J. Biol. Chem.* 277(25), 22353–22360 (2002).

44 Young JD, Lowrey DM. Biochemical and functional characterization of a membrane-associated pore-forming protein from the pathogenic ameboflagellate *Naegleria fowleri*. *J. Biol. Chem.* 264(2), 1077–1083 (1989).

45 Jamerson M, Da Rocha-Azevedo B, Cabral GA, Marciano-Cabral F. Pathogenic *Naegleria fowleri* and nonpathogenic *Naegleria lovaniensis* exhibit differential adhesion to, and invasion of, extracellular matrix proteins. *Microbiology* 158(Pt 3), 791–803 (2012).

46 Ramírez-Rico G, Martínez-Castillo M, De La Garza M, Shibayama M, Serrano-Luna J. *Acanthamoeba castellanii* proteases are capable of degrading iron-binding proteins as a possible mechanism of pathogenicity. *J. Eukaryot. Microbiol.* 62(5), 614–622 (2015).

47 Luna-Castro S, Aguilar-Romero F, Samaniego-Barron L, Godinez-Vargas D, de la Garza M. Effect of bovine apo-lactoferrin on the growth and virulence of *Actinobacillus pleuropneumoniae*. *Biometals.* 27(5), 891–903 (2014).

48 Verma S, Dixit R, Pandey KC. Cysteine proteases: modes of activation and future prospects as pharmacological targets. *Front. Pharmacol.* 7, 107 (2016).

49 Sajid M, Mckerrow JH. Cysteine proteases of parasitic organisms. *Mol. Biochem. Parasitol.* 120(1), 1–21 (2002).

50 Mottram JC, Helms MJ, Coombs GH, Sajid M. Clan CD cysteine peptidases of parasitic protozoa. *Trends Parasitol.* 19(4), 182–187 (2003).

51 Barrett AJ. Classification of peptidases. *Methods Enzymol.* 244, 1–15 (1994).

52 Cotta MA, Hespell RB. Proteolytic activity of the ruminal bacterium *Butyrivibrio fibrisolvens*. *Appl. Environ. Microbiol.* 52(1), 51–58 (1986).

53 Avila M, Jaquet M, Moine D *et al.* Physiological and biochemical characterization of the two alpha-L-rhamnosidases of *Lactobacillus plantarum* NCC245. *Microbiology* 155(Pt 8), 2739–2749 (2009).

54 Hebraud M, Fevre M. Purification and characterization of an extracellular beta-xylosidase from the rumen anaerobic fungus *Neocallimastix frontalis*. *FEMS Microbiol. Lett.* 60(1–2), 11–16 (1990).

55 Tiwari P, Misra BN, Sangwan NS. Beta-glucosidases from the fungus trichoderma: an efficient cellulase machinery in biotechnological applications. *Biomed. Res. Int.* 203735 (2013).

• **Contains evidence of glycosidases inhibition by p-hydroxymercuribenzoate.**

56 Chadee K, Keller K, Forstner J, Innes DJ, Ravdin JI. Mucin and nonmucin secretagogue activity of *Entamoeba histolytica* and cholera toxin in rat colon. *Gastroenterology* 100(4), 986–997 (1991).

57 Olomu N, Martinez AJ, Lamarco KL *et al.* Demonstration of various acid hydrolases and preliminary characterization of acid phosphatase in *Naegleria fowleri*. *J. Protozool.* 33(3), 317–321 (1986).

58 Fritz-Laylin LK, Ginger ML, Walsh C, Dawson SC, Fulton C. The *Naegleria* genome: a free-living microbial eukaryote lends unique insights into core eukaryotic cell biology. *Res. Microbiol.* 162(6), 607–618 (2011).

59 Moncada DM, Kammanadiminti SJ, Chadee K. Mucin and Toll-like receptors in host defense against intestinal parasites. *Trends Parasitol.* 19(7), 305–311 (2003).

60 Irwin JA, Morrissey PE, Ryan JP *et al.* Glycosidase activity in the excretory-secretory products of the liver fluke, *Fasciola hepatica*. *Parasitology* 129(Pt 4), 465–472 (2004).

61 Das S, Saha AK, Nerad TA *et al.* Partial purification and characterization of *Naegleria fowleri* beta-glucosidase. *J. Protozool.* 34(1), 68–74 (1987).

•• **Demonstrated the presence of β-glucosidase in total crude extracts of *N. fowleri*.**

62 Eisen D, Franson RC. Acid-active neuraminidases in the growth media from cultures of pathogenic *Naegleria fowleri* and in sonicates of rabbit alveolar macrophages. *Biochim. Biophys. Acta* 924(2), 369–372 (1987).

63 Hounsell EF. Physicochemical analyses of oligosaccharide determinants of glycoproteins. *Adv. Carbohydr. Chem. Biochem.* 50, 311–350 (1994).

64 Perez-Vilar J, Randell SH, Boucher RC. C-mannosylation of MUC5AC and MUC5B Cys subdomains. *Glycobiology* 14(4), 325–337 (2004).

65 Ozeki T, Yosizawa Z. Glycopeptides isolated from bovine submaxillary mucin. *Arch. Biochem. Biophys.* 142(1), 177–183 (1971).

66 Tsuji T, Osawa T. Carbohydrate structures of bovine submaxillary mucin. *Carbohydr. Res.* 151, 391–402 (1986).

•• **Demonstrated the type of carbohydrates present in the bovine submaxillary mucin.**

67 Hashimoto Y, Pigman W. Comparison of composition of mucins and blood-group substances. *Ann. NY Acad. Sci.* 93(12), 541–554 (1962).

68 Kratz A, Lewandrowski KB. Case records of the Massachusetts General Hospital. Weekly clinicopathological exercises. Normal reference laboratory values. *N. Engl J. Med.* 339(15), 1063–1072 (1998).

69 Kardar G, Oraei M, Shahsavani M *et al.* Reference intervals for serum immunoglobulins IgG, IgA, IgM and complements C3 and C4 in Iranian healthy children. *Iran J. Public Health* 41(7), 59–63 (2012).

70 Ferrante A, Thong YH. Antibody induced capping and endocytosis of surface antigens in *Naegleria fowleri*. *Int. J. Parasitol.* 9(6), 599–601 (1979).